

# Effect of spin diffusion on Gilbert damping for a very thin permalloy layer in Cu/permalloy/Cu/Pt films

著者	安藤 康夫
journal or publication title	Physical review. B
volume	66
number	10
page range	104413-1-104413-9
year	2002
URL	<a href="http://hdl.handle.net/10097/35855">http://hdl.handle.net/10097/35855</a>

doi: 10.1103/PhysRevB.66.104413

## Effect of spin diffusion on Gilbert damping for a very thin permalloy layer in Cu/permalloy/Cu/Pt films

S. Mizukami,\* Y. Ando, and T. Miyazaki

*Department of Applied Physics, Graduate School of Engineering, Tohoku University, Aoba-yama 05, Sendai, Japan*

(Received 11 March 2002; revised manuscript received 18 June 2002; published 16 September 2002)

Ferromagnetic resonance (FMR) was measured for Cu/permalloy (Py) (20, 30, 40 Å)/Cu ( $d_{\text{Cu}}$ )/Pt (0, 50 Å) films with various  $d_{\text{Cu}}$  to clarify the effect of spin diffusion driven by the precession of magnetization on Gilbert damping. The peak-to-peak linewidth  $\Delta H_{pp}$  of the FMR spectra for Cu/Py/Cu/Pt films was very large at  $d_{\text{Cu}}=0$  Å, and decreased remarkably at  $d_{\text{Cu}}=30$  Å. Above  $d_{\text{Cu}}=30$  Å, it decreased gradually with increasing  $d_{\text{Cu}}$  in the anomalously wide range of  $d_{\text{Cu}}$ . The out-of-plane angular dependence of the FMR of Cu/Py(30 Å)/Cu ( $d_{\text{Cu}}$ )/Pt (0, 50 Å) films was measured and analyzed using a Landau-Lifshitz-Gilbert equation that took into account the local variation of the effective demagnetizing field. The Gilbert damping coefficient  $G$  obtained from the analysis for Cu/Py/Cu/Pt films was about twice as large as that for Cu/Py/Cu films even at  $d_{\text{Cu}}=100$  Å and decreased gradually as  $d_{\text{Cu}}$  increased. At  $d_{\text{Cu}}=2000\text{--}3000$  Å,  $G$  for Cu/Py/Cu/Pt and Cu/Py/Cu films has the same value. We discussed the influence of spin diffusion driven by the precession of magnetization in FMR on  $G$  using a previously proposed model. The calculated  $G$  vs  $d_{\text{Cu}}$  fitted well to the experimental one, and the other features of the experimental results are well explained by the model.

DOI: 10.1103/PhysRevB.66.104413

PACS number(s): 75.70.-i, 76.50.+g, 72.25.Mk, 72.25.Rb

### I. INTRODUCTION

Recently, it has been predicted theoretically that a spin-polarized current can excite spin wave or drive the reversal of magnetization in a very thin ferromagnetic metal (FM) layer involved in a FM/normal metal (NM)/FM film.<sup>1,2</sup> Many groups have examined the prediction experimentally,<sup>3</sup> as it is expected to be applicable to magnetoelectronics, such as the magnetic random access memory.<sup>2</sup> Furthermore, Berger has suggested that the inverse effects can also appear in FM/NM/FM films, such as spin accumulation induced by the precession of magnetization in the ferromagnetic resonance (FMR).<sup>1,4</sup> For a full understanding of the effects of spin-polarized current on the dynamics of magnetization, study of such inverse effects is important.

A similar inverse effect has been studied in FM/NM bilayers using conduction-electron spin resonance (CESR) combined with FMR.<sup>5-7</sup> Silsbee *et al.* suggested that the precession of magnetization for a FM layer can drive conduction spin diffusion at the FM/NM interface.<sup>6</sup> If the thickness of the FM layer is sufficiently thin, it can be expected that spin diffusion driven by the precession of magnetization in FMR also influences the dynamics of magnetization for the FM layer, particularly the magnetic damping, in a NM/FM/NM film. Intrinsic magnetic damping, so-called Gilbert damping, has been extensively investigated for bulk or FM film using measurements of the linewidth and the line shape of FMR spectrum,<sup>8,10,9,11</sup> while no studies of a similar nature have been reported of Gilbert damping for a thin FM layer.

To clarify the effect of spin diffusion on Gilbert damping for a very thin FM layer, we studied the linewidth of FMR for a thin Ni<sub>80</sub>Fe<sub>20</sub> permalloy (Py) layer in NM/Py/NM films (NM=Cu, Ta, Pd, and Pt).<sup>12,13</sup> In this study, it has been found that Gilbert damping coefficient  $G$  increased when NM=Pt or Pd, and was almost unchanged for NM=Cu or Ta. For bulk FM, the magnitude of  $G$  is considered to depend

on that of the spin-orbit coupling,<sup>14</sup> so it is unclear whether spin diffusion is responsible for the enhancement of  $G$  for Pt/Py/Pt or Pd/Py/Pd films. Therefore, we studied the linewidth of FMR for Cu/Py/Cu/Pt films with various Cu spacer layer thicknesses to examine the effect of spin diffusion on  $G$  for a very thin Py film. The experimental results have already been briefly reported.<sup>15</sup> In this paper, we describe the experimental data in detail and discuss  $G$  for Cu/Py/Cu/Pt films using the phenomenological model proposed by Silsbee *et al.*<sup>6</sup>

### II. EXPERIMENTAL PROCEDURE

Films were prepared by magnetron sputtering on the substrate of Corning 7059 glass cooled by water. The base pressure was less than  $5 \times 10^{-7}$  Torr, and Ar pressure was 7 mTorr. Cu/Py ( $d_{\text{Py}}$ )/Cu ( $d_{\text{Cu}}$ )/Pt (50 Å) films were systematically fabricated with varying  $d_{\text{Py}}$  and  $d_{\text{Cu}}$ . We also fabricated Cu/Py ( $d_{\text{Py}}$ )/Cu ( $d_{\text{Cu}}$ ) films and Cu/Py ( $d_{\text{Py}}$ )/Cu (50 Å)/Cu (50 Å)/Pt (50 Å) films as control samples. In fabricating Cu/Py ( $d_{\text{Py}}$ )/Cu (50 Å)/Cu (50 Å)/Pt (50 Å) films, the films were exposed to air after sputtering the first 50 Å Cu spacer layer. In addition, Cu/Py (30 Å)/Cu (100 Å)/Pt ( $d_{\text{Pt}}$ )/Cu (50 Å) films were also prepared with various  $d_{\text{Pt}}$ . The thickness of the Cu buffer layer was 50 Å for all samples. FMR was measured using a X-band (9.77 GHz) electron-spin-resonance spectrometer and a TE 102 cavity. For measurements of the out-of-plane angular dependence of FMR, the sample was fixed on a quartz rod, and a goniometer was used to vary the angle. Magnetization measurements were carried out by a superconducting quantum interference device magnetometer. The surface morphology of the films was measured using an atomic force microscope.

### III. METHOD OF ANALYSIS OF THE OUT-OF-PLANE ANGULAR DEPENDENCE OF FMR

The linewidth of FMR reflects not only  $G$  but also the magnetic inhomogeneities in a film, such as the local varia-

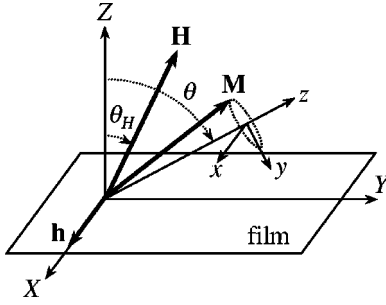


FIG. 1. The coordinate system used for measurement and analysis of the out-of-plane angular dependence of FMR.

tion of magnetic anisotropy, the so-called anisotropy dispersion. In order to evaluate  $G$  for the films from the linewidth of FMR, we carried out measurements and numerical analyses of the out-of-plane angular dependence of FMR,<sup>16,17,11–13</sup> which is based on the Landau-Lifshitz-Gilbert (LLG) equation,<sup>8</sup>

$$-\frac{1}{\gamma} \frac{d\mathbf{M}}{dt} = \mathbf{M} \times (\mathbf{H}_{\text{eff}} + \mathbf{h}) - \frac{\alpha}{\gamma M_S} \mathbf{M} \times \frac{d\mathbf{M}}{dt}. \quad (1)$$

Here  $\mathbf{M}$ ,  $\mathbf{H}_{\text{eff}}$ ,  $\mathbf{h}$ , and  $M_S$  are the vectors of the magnetization, the effective magnetic field acting on  $\mathbf{M}$ , the external microwave field, and the saturation magnetization, respectively.  $\gamma$  and  $\alpha$  are the gyromagnetic ratio and the dimensionless damping coefficient, defined as  $\gamma \equiv g \mu_B / \hbar$  and  $\alpha \equiv G / \gamma M_S$ , respectively. Here,  $g$ ,  $\mu_B$ , and  $\hbar$  are the  $g$  factor, the Bohr magneton number, and the Planck constant, respectively. We took into account the external dc magnetic field, the demagnetizing field, and the perpendicular anisotropy field as  $\mathbf{H}_{\text{eff}}$ . The coordinate system is as in Fig. 1. The vector of the external dc magnetic field  $\mathbf{H}$  lies in the  $Y$ - $Z$  plane, and its direction is defined by  $\theta_H$ .  $\mathbf{h}$  is parallel to the  $X$  direction and is written as

$$\mathbf{h} = \delta h e^{-i\omega t} \hat{\mathbf{x}}. \quad (2)$$

Here,  $\omega = 2\pi f$ , and  $f$  is the microwave frequency. The small precession of  $\mathbf{M}$  around the equilibrium direction is taken as a solution of Eq. (1), which is given as

$$\mathbf{M} = \delta M_x e^{-i\omega t} \hat{\mathbf{x}} + \delta M_y e^{-i\omega t} \hat{\mathbf{y}} + M_S \hat{\mathbf{z}}. \quad (3)$$

Here, the  $z$  axis is taken to be the equilibrium direction defined by  $\theta$ . The  $y$ - $z$  plane lies in the  $Y$ - $Z$  plane, and the  $x$  axis is identical to the  $X$  axis. Substituting Eqs. (2) and (3) into Eq. (1), one obtains the resonance condition of the FMR on the linear approximation, which is given by the following relations,<sup>16,12</sup>

$$\omega / \gamma = \sqrt{H_1 H_2}, \quad (4)$$

$$H_1 = H_{res} \cos(\theta_H - \theta) - 4\pi M_{\text{eff}} \cos 2\theta, \quad (5)$$

$$H_2 = H_{res} \cos(\theta_H - \theta) - 4\pi M_{\text{eff}} \cos^2 \theta. \quad (6)$$

Here,  $H_{res}$  is the resonance field and  $4\pi M_{\text{eff}}$  is the effective demagnetizing field defined as  $4\pi M_{\text{eff}} \equiv 4\pi M_S - 2K_{\perp} / M_S$ ,

with the perpendicular magnetic anisotropy constant  $K_{\perp}$ .  $\theta$  is obtained from the following equation:

$$2H_{res} \sin(\theta - \theta_H) = 4\pi M_{\text{eff}} \sin 2\theta. \quad (7)$$

One also obtains the full width at half maximum (FWHM) of a FMR spectrum caused intrinsically by Gilbert damping from Eq. (1), which is expressed as<sup>16,12</sup>

$$\Delta H_{\text{in}} = \alpha (H_1 + H_2) \left| \frac{d(\omega / \gamma)}{dH_{res}} \right|^{-1}. \quad (8)$$

We assume that the FWHM due to the anisotropy dispersion for the out-of-plane direction is expressed as<sup>17,11,12</sup>

$$\Delta H_{\text{ex}} = \left| \frac{dH_{res}}{d(4\pi M_{\text{eff}})} \right| \Delta(4\pi M_{\text{eff}}) + \left| \frac{dH_{res}}{d\theta_H} \right| \Delta\theta_H. \quad (9)$$

Here,  $\Delta(4\pi M_{\text{eff}})$  and  $\Delta\theta_H$  represent the dispersion of the magnitude and the direction of  $4\pi M_{\text{eff}}$ , respectively. Equation (9) states that the extrinsic linewidth  $\Delta H_{\text{ex}}$  is caused by the local variation of the magnitude and the direction of  $4\pi M_{\text{eff}}$  through the local variation of  $H_{res}$ . The influence of the anisotropy dispersion parallel to a film plane on  $\Delta H_{\text{ex}}$  is not taken into account since it is considered to be small for Py films.<sup>18</sup> The peak-to-peak linewidth  $\Delta H_{pp}$  is assumed to be expressed as<sup>17,11,12</sup>

$$\Delta H_{pp} = \Delta H_{\text{in}} / \sqrt{3} + \Delta H_{\text{ex}} / \sqrt{3}. \quad (10)$$

Here, the multiplying of  $1/\sqrt{3}$  is the correction of the difference between the FWHM and the peak-to-peak linewidth for the line shape of Lorentzian.  $H_{res}$  vs  $\theta_H$  is calculated using Eqs. (4)–(7) numerically, and is fitted to the experimental  $H_{res}$  vs  $\theta_H$  by adjusting the value of  $g$  and  $4\pi M_{\text{eff}}$ .  $\Delta H_{pp}$  vs  $\theta_H$  is also calculated from Eqs. (4)–(10) numerically, using  $g$  and  $4\pi M_{\text{eff}}$  obtained from the fitting of  $H_{res}$  vs  $\theta_H$ , and is fitted to the experimental  $\Delta H_{pp}$  vs  $\theta_H$  by adjusting the value of  $\alpha$ ,  $\Delta(4\pi M_{\text{eff}})$ , and  $\Delta\theta_H$ . It is noted that the multiplying of  $1/\sqrt{3}$  for the second term of Eq. (10) has been omitted in other papers.<sup>11,17</sup> Since the spectra for our films were Lorentzian except for  $\theta_H \approx 0^\circ$ , we assumed the multiplying of  $1/\sqrt{3}$ . However, the value of  $\alpha$  evaluated from the fitting does not depend on this assumption.

#### IV. EXPERIMENTAL RESULTS

Figure 2(a) shows the examples of FMR spectra measured at  $\theta_H = 90^\circ$  for Cu/Py (30 Å)/Cu ( $d_{\text{Cu}}$ )/Pt films with various  $d_{\text{Cu}}$ . The spectra are normalized and are shown as a function of the external dc magnetic field around  $H_{res}$ . Although the spectra for  $d_{\text{Cu}} = 0$  and 30 Å are slightly asymmetric, the spectra keep the line shape of a Lorentzian for all  $d_{\text{Cu}}$ . Figure 2(b) shows the spectra for Cu/Py (30 Å)/Cu (100 Å)/Pt and Cu/Py (30 Å)/Cu (100 Å) films in the same manner as that in Fig. 2(a). The calculated Lorentzian curves are shown in Fig. 2(b) with the solid lines. Lorentzian curves fit the experimental data almost completely for both the films. It is unlikely that the difference of  $\Delta H_{pp}$  between the films with and without the Pt layer is due to the increase of anisotropy dispersion in a film, because if the anisotropy dispersion

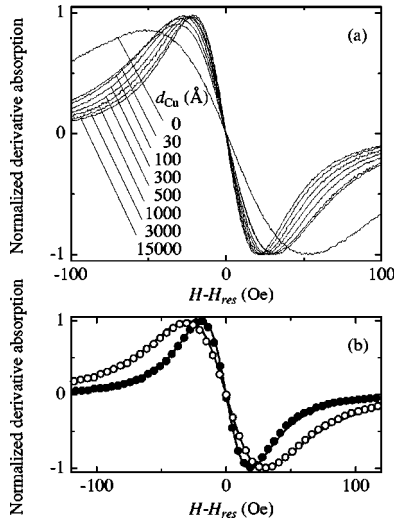


FIG. 2. (a) Normalized FMR spectra measured at  $\theta_H=90^\circ$  for Cu/Py (30 Å)/Cu ( $d_{Cu}$ )/Pt films with various  $d_{Cu}$ . Horizontal axis is the external dc magnetic field measured from  $H_{res}$ . (b) Normalized FMR spectra measured at  $\theta_H=90^\circ$  for Cu/Py (30 Å)/Cu (100 Å)/Pt film (open circles) and Cu/Py (30 Å)/Cu (100 Å) film (solid circles). Lines are the calculated Lorentzian curves and are fitted to the experimental data. The experimental data points are thinned for easier viewing.

were to increase  $\Delta H_{pp}$  dominantly through the local variation of  $H_{res}$ , the line shape would tend to become Gaussian-like or a heavily distorted line shape.<sup>19</sup> In addition, we note that the shapes of the magnetization curves for these films are same.

Figures 3(a) and 3(b) show  $d_{Cu}$  dependence of  $\Delta H_{pp}$  for Cu/Py ( $d_{Py}$ )/Cu ( $d_{Cu}$ )/Pt (0,50 Å) films with various  $d_{Py}$  in the thinner regime of  $d_{Cu}$  and in the full range of  $d_{Cu}$ , respectively.  $\Delta H_{pp}$  was obtained from the FMR spectra measured at  $\theta_H=90^\circ$ . As seen in Fig. 3(a),  $\Delta H_{pp}$  for Cu/Py/Cu/Pt film is rather large at  $d_{Cu}=0$  Å. Such a large  $\Delta H_{pp}$  has also been observed for Pt/Py/Pt film.<sup>12,13</sup> By inserting a 30 Å thick Cu spacer layer,  $\Delta H_{pp}$  drops remarkably, implying that the large increase of  $\Delta H_{pp}$  requires the intimate contact of the Pt layer. While,  $\Delta H_{pp}$  for Cu/Py/Cu/Pt film is still larger than that for the films without the Pt layer, and decreases gradually for a wide range of  $d_{Cu}$ , as shown in Fig. 3(b),  $\Delta H_{pp}$  for Cu/Py/Cu films increases slightly with increasing  $d_{Cu}$ .  $\Delta H_{pp}$  for the films with and without the Pt layer becomes almost the same at  $d_{Cu}=2000$ – $3000$  Å. With decreasing  $d_{Py}$ , the difference of  $\Delta H_{pp}$  between those films increases in the thin regime of  $d_{Cu}$ . On the other hand,  $H_{res}$  is independent of  $d_{Cu}$  and is not influenced by the Pt layer.

Figure 4 shows  $\Delta H_{pp}$  for Cu/Py (30 Å)/Cu (100 Å)/Pt ( $d_{Pt}$ )/Cu films as a function of  $d_{Pt}$ .  $\Delta H_{pp}$  was obtained from the FMR spectra measured at  $\theta_H=90^\circ$ .  $\Delta H_{pp}$  increases rapidly in the very thin regime of  $d_{Pt}$  and saturates at  $d_{Pt} \approx 10$  Å. This thickness is supposedly the thickness at which the Pt islands become a continuous layer and entirely cover the surface of the Cu layer. This result implies that the increase of  $\Delta H_{pp}$  for Cu/Py/Cu/Pt film requires only the interface between the Cu and the Pt layer.

We measured the out-of-plane angular dependence of

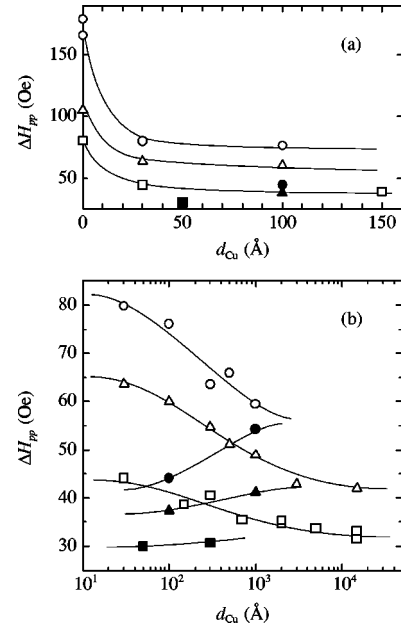


FIG. 3.  $d_{Cu}$  dependence of the peak-to-peak linewidth  $\Delta H_{pp}$  (a) in the thinner regime of  $d_{Cu}$  and (b) in the full range of  $d_{Cu}$  for Cu/Py ( $d_{Py}$ )/Cu ( $d_{Cu}$ )/Pt ( $d_{Pt}$ ) films. Data were obtained from the FMR spectra measured at  $\theta_H=90^\circ$ . The open and the solid symbols correspond to the data for  $d_{Pt}=50$  and  $0$  Å, respectively.  $\circ$  ( $\bullet$ ),  $\blacktriangle$  ( $\triangle$ ), and  $\blacksquare$  ( $\square$ ) represent the data for  $d_{Py}=20, 30$ , and  $40$  Å, respectively. Lines are visual guides.

FMR for Cu/Py (30 Å)/Cu ( $d_{Cu}$ )/Pt (0, 50 Å) films. Figures 5(a) and 5(b) show examples of the out-of-plane angular dependence of  $\Delta H_{pp}$  and  $H_{res}$  for Cu/Py/Cu (100 Å) and Cu/Py/Cu (100 Å)/Pt films, respectively.  $\Delta H_{pp}$  vs  $\theta_H$  and  $H_{res}$  vs  $\theta_H$  exhibit strong peaks at  $\theta_H \approx 15^\circ$  and  $\theta_H=0^\circ$ , respectively. The peak of  $\Delta H_{pp}$  at  $\theta_H \approx 15^\circ$  is because of the increase of the linewidth due to Gilbert damping.<sup>16,12,13</sup> The peak of  $H_{res}$  at  $\theta_H=0^\circ$  is caused by the demagnetizing field that is operatively strong at this angle. In the data of  $\Delta H_{pp}$  vs  $\theta_H$  for both films, another small peak is also found at  $\theta_H=0^\circ$ . This small peak is due to the dispersion of the magnitude of  $4\pi M_{eff}$ , which is also effective at this angle.<sup>12,13,16</sup> The data of  $H_{res}$  vs  $\theta_H$  in the insets of Figs. 5(a) and 5(b) are nearly the same, indicating that  $g$  and  $4\pi M_{eff}$  are same between the two films. On the other hand,  $\Delta H_{pp}$  for Cu/Py/Cu (100 Å)/Pt film is larger than that for the film without the Pt

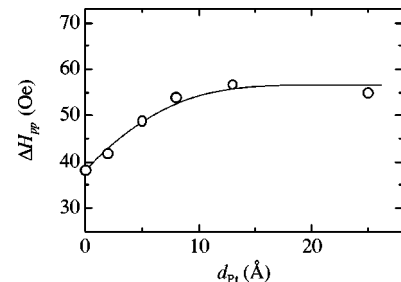


FIG. 4.  $d_{Pt}$  dependence of  $\Delta H_{pp}$  for Cu/Py (30 Å)/Cu (100 Å)/Pt ( $d_{Pt}$ )/Cu films.  $\Delta H_{pp}$  was obtained from the FMR spectra measured at  $\theta_H=90^\circ$ . The line is a visual guide.



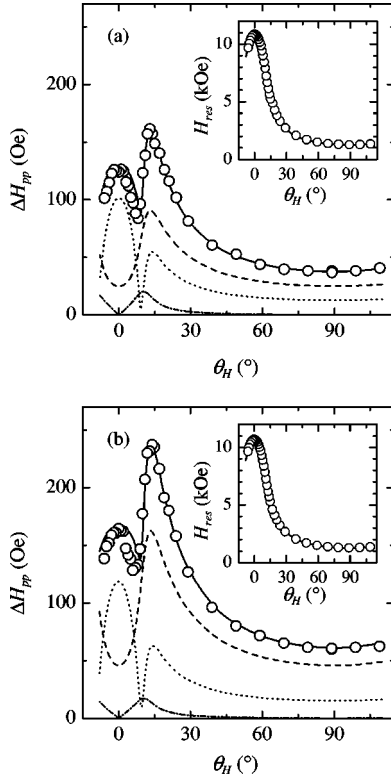


FIG. 5. The out-of-plane angular dependence of  $\Delta H_{pp}$  for (a) Cu/Py (30 Å)/Cu (100 Å) and (b) Cu/Py (30 Å)/Cu (100 Å)/Pt film, respectively. Insets show the out-of-plane angular dependence of  $H_{res}$ . Open circles represent the experimental data and are fitted to the experimental ones. Solid lines are the calculated data and are fitted to the experimental ones. Broken, dotted, and dotted-and-broken lines are the three components of the calculated  $\Delta H_{pp}$ . The best-fitted parameters are  $g=2.11$ ,  $4\pi M_{\text{eff}}=7.5$  kG,  $\alpha=0.0065$ ,  $\Delta(4\pi M_{\text{eff}})=175$  G, and  $\Delta\theta_H=0.057^\circ$  for Cu/Py (30 Å)/Cu (100 Å) and  $g=2.11$ ,  $4\pi M_{\text{eff}}=7.4$  kG,  $\alpha=0.012$ ,  $\Delta(4\pi M_{\text{eff}})=205$  G, and  $\Delta\theta_H=0.052^\circ$  for Cu/Py (30 Å)/Cu (100 Å)/Pt, respectively.

layer in the full range of  $\theta_H$ . The increase of  $\Delta H_{pp}$  in the full range of  $\theta_H$  cannot be explained by two-magnon scattering, because the linewidth due to two-magnon scattering is zero around  $\theta_H=0^\circ$ .<sup>20</sup> To our knowledge, such an increase of  $\Delta H_{pp}$  is only explainable by the increasing of  $\alpha$ .<sup>12,13</sup>

The experimental data of  $H_{res}$  vs  $\theta_H$  and  $\Delta H_{pp}$  vs  $\theta_H$  were analyzed using the method described in Sec. III. The examples of the results of fitting are shown in Figs. 5(a) and 5(b) with the solid lines. The calculated data are well fitted to the experimental data for  $\Delta H_{pp}$  and  $H_{res}$ . Three components of the calculated  $\Delta H_{pp}$ , which are  $\Delta H_{\text{in}}/\sqrt{3}$  and the first and the second terms of  $\Delta H_{\text{ex}}/\sqrt{3}$ , are shown in Figs. 5(a) and 5(b) with the broken, the dotted and the dotted-and-broken lines, respectively. The magnitudes of these three components of  $\Delta H_{pp}$  are proportional to  $\alpha$ ,  $\Delta(4\pi M_{\text{eff}})$ , and  $\Delta\theta_H$  from Eqs. (8) and (9). Therefore,  $\Delta(4\pi M_{\text{eff}})$  and  $\Delta\theta_H$  are almost the same between the two films, and only  $\alpha$  is significantly different.

Analysis of the other films showed that only  $\alpha$  systematically depended on  $d_{\text{Cu}}$  and the presence of the Pt layer. The value of  $g$  for these films was about 2.11, which agreed with

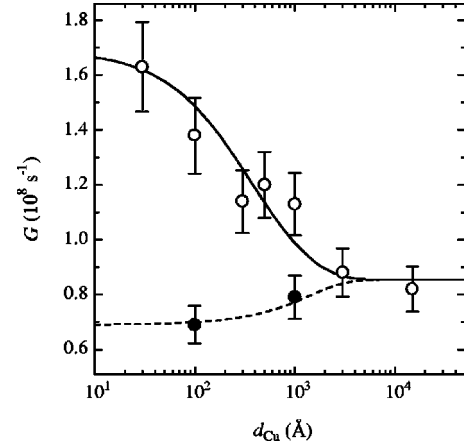


FIG. 6.  $d_{\text{Cu}}$  dependence of Gilbert damping coefficient  $G$  for Cu/Py (30 Å)/Cu ( $d_{\text{Cu}}$ )/Pt films (open circle) and Cu/Py (30 Å)/Cu ( $d_{\text{Cu}}$ ) films (solid circle). Lines are the calculated data and are fitted to the experimental ones using Eqs. (25), (33), and (34) with  $G_{\text{Py}}=0.69 \times 10^8 \text{ s}^{-1}$ ,  $\chi_p=9.8 \times 10^{-7}$  (in cgs unit),  $D_p=120 \text{ cm}^2/\text{s}$ ,  $l_p=2000 \text{ Å}$ , and  $\Gamma=30 \text{ cm/s}$ . Solid and broken lines correspond to  $\alpha_S^{-1} \rightarrow 0$  and  $\alpha_S=0$ , respectively.

another reported value.<sup>21</sup> The value of  $4\pi M_{\text{eff}}$  was found to be about 7.5 kG. This value is almost same as the average value of  $4\pi M_S \approx 7.2$  kG for these films, so that  $K_{\perp}$  is negligible for the films, and this agrees with other reports.<sup>22</sup> No dependences of  $\Delta(4\pi M_{\text{eff}})$  or  $\Delta\theta_H$  on  $d_{\text{Cu}}$  and the presence of the Pt layer are also reasonable findings, because  $\Delta(4\pi M_{\text{eff}})$  and  $\Delta\theta_H$  for a thin Py layer are considered to be due to the local fluctuation of  $d_{\text{Py}}$  and the waviness of the Py layer,<sup>12</sup> and such structural imperfections cannot be influenced by an overlayer structure.

Figure 6 shows  $G$  for Cu/Py (30 Å)/Cu ( $d_{\text{Cu}}$ )/Pt and Cu/Py (30 Å)/Cu ( $d_{\text{Cu}}$ ) films as a function of  $d_{\text{Cu}}$ . The value of  $G$  was evaluated from  $\alpha$  using  $g$  and  $M_S$  for each film. The errors in  $G$  are mostly due to the uncertainties of  $M_S$ . The trend of  $G$  for Cu/Py/Cu ( $d_{\text{Cu}}$ )/Pt and Cu/Py/Cu ( $d_{\text{Cu}}$ ) films is similar to that of  $\Delta H_{pp}$  shown in Fig. 3(b). In the thin region of  $d_{\text{Cu}}$ ,  $G$  for Cu/Py/Cu/Pt films is found to be about two times larger than that for films without the Pt layer.  $G$  for Cu/Py/Cu/Pt films decreases monotonically with increasing  $d_{\text{Cu}}$ .  $G$  for Cu/Py/Cu films is close to the bulk value of  $G$  for Py in Ref. 23 at  $d_{\text{Cu}}=100 \text{ Å}$  and increases slightly as  $d_{\text{Cu}}$  increases.  $G$  for both films becomes equal at  $d_{\text{Cu}}=2000\text{--}3000 \text{ Å}$ .

## V. DISCUSSION

The large  $\Delta H_{pp}$  for Cu/Py/Pt films in Fig. 3(a) or  $G$  for Pt/Py/Pt films in Refs. 12 and 13 can be explained qualitatively by theories for Gilbert damping for bulk FM.<sup>14</sup> Similar explanations have been made for the enhancement of  $G$  in epitaxial Fe and Ni ultrathin films.<sup>10,11</sup> However, the rapid decrease of  $\Delta H_{pp}$  in Fig. 3(a) implies that such an explanation is difficult for Cu/Py/Cu/Pt films, and some other mechanism should be taken into consideration for the explanation of the enhancement of  $G$  for these films. In discussing the mechanism of the enhancement of  $G$  for Cu/Py/Cu/Pt

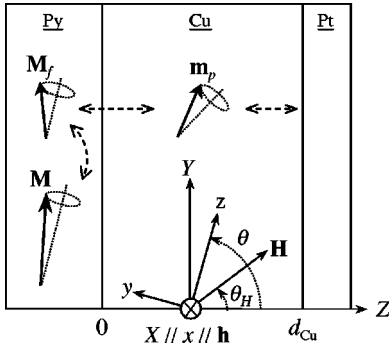


FIG. 7. A schematic illustration of the coordinate system used in the discussion.

films, we note that the enhancement of  $G$  was not observed for Cu/Py/Cu/Cu/Pt films. This means that the enhancement of  $G$  for Cu/Py/Cu/Pt films is caused by some mediation inside the Cu spacer layer. The mediation of the Ruderman-Kittel-Kasuya-Yosida-like spin polarization is excluded because it is known to be limited near the Py/Cu interface.<sup>24</sup> It is also difficult to consider that the enhancement of  $G$  is due to the pinholes or the diffusion of Pt atoms, because the Cu spacer layer is thick enough, and its surface is smooth from the AFM measurements. We consider that this long-range effect is related to the spin diffusion of the conduction electron in the Cu spacer layer, since the conduction electron can diffuse for a long distance in a Cu layer without losing its spin memory.<sup>25,26</sup> The spin diffusion can be driven by the precession of magnetization in FMR, as mentioned in Sec. I.<sup>6</sup> The enhancement of  $G$  for Cu/Py/Cu/Pt films is discussed from such a point of view, based on the phenomenological model proposed by Silsbee *et al.*<sup>6</sup>

The schematic illustration for this discussion is shown in Fig. 7. For simplicity, we neglect the effect of the Cu buffer layer.  $\mathbf{M}$  is the vector of the magnetic moment per unit volume for the localized electron spins in the Py layer.  $\mathbf{M}_f$  and  $\mathbf{m}_p$  are those for the conduction-electron spins in the Py layer and the Cu layer, respectively.  $\mathbf{H}$ ,  $\mathbf{h}$ , the  $X$ - $Y$ - $Z$  coordinate, and the  $x$ - $y$ - $z$  one are defined the same as those in Fig. 1. The dynamics of  $\mathbf{M}$  are described by

$$-\frac{1}{\gamma_F} \frac{d\mathbf{M}}{dt} = \mathbf{M} \times (\mathbf{H}_{\text{eff}} + \mathbf{h}) - \frac{G_F}{(\gamma_F M_S)^2} \mathbf{M} \times \frac{d\mathbf{M}}{dt} + \mathbf{T}, \quad (11)$$

where  $\gamma_F$  is the gyromagnetic ratio and  $G_F$  is the Gilbert damping coefficient for the localized electron spins. We regard  $\mathbf{M}$  and  $\mathbf{H}_{\text{eff}}$  to be the same as those in Eq. (1), since the magnetization  $M_f$  of the conduction-electron spins is much smaller than that of the localized electron spins. We use Gilbert's expression as the magnetic damping term, namely, the second term of Eq. (11). In Ref. 6, Bloch's expression was used, while Gilbert's expression is appropriate for describing the magnetic damping for the strongly coupled spins.<sup>27</sup> We assume that the torque by the exchange interaction of  $\mathbf{M}_f$  is expressed as

$$\mathbf{T} = \mathbf{M} \times \lambda \mathbf{M}_f, \quad (12)$$

where  $\lambda$  is the molecular field coefficient, and  $\mathbf{T}$ , which had been neglected in Ref. 6, is essential for our discussion. In the case of  $\mathbf{T} = 0$ , Eq. (11) is identical to Eq. (1) by taking  $\gamma = \gamma_F$  and  $G = G_F$ , namely, the dynamics of the magnetization are determined only by the nature of the localized electron spins. The dynamics of  $\mathbf{M}_f$  are assumed to be expressed as

$$\frac{d\mathbf{M}_f}{dt} = -\gamma_f \mathbf{M}_f \times \lambda \mathbf{M} - \frac{\mathbf{M}_f - \chi_f \lambda \mathbf{M}}{\tau_f} - \frac{\mathbf{J}_f}{d_{\text{Py}}}. \quad (13)$$

Here,  $\gamma_f$ ,  $\chi_f$ , and  $\tau_f$  are the gyromagnetic ratio, Pauli paramagnetic susceptibility, and the spin-relaxation time for the conduction electron in the Py layer, respectively.  $\mathbf{J}_f$  is the current density of the spin magnetic moment diffusing out of the Py layer at the Py/Cu interface. We do not treat the spatial variation of  $\mathbf{M}_f$  inside the Py layer. The molecular field of the exchange interaction  $\lambda \mathbf{M}$  is taken only into account as the effective magnetic field. The dynamics and the transport of  $\mathbf{m}_p$  are well described by the Bloch-Torrey equation,<sup>6,28</sup>

$$\frac{\partial \mathbf{m}_p}{\partial t} = -\gamma_p \mathbf{m}_p \times \mathbf{H} - \frac{\mathbf{m}_p - \chi_p \mathbf{H}}{\tau_p} + D_p \frac{\partial^2}{\partial Z^2} (\mathbf{m}_p - \chi_p \mathbf{H}). \quad (14)$$

$\gamma_p$ ,  $\chi_p$ , and  $\tau_p$  denote the same as those of  $\mathbf{M}_f$ .  $D_p$  is the diffusion coefficient for the conduction electron in the Cu layer. We neglect any other magnetic field acting on  $\mathbf{m}_p$  except for  $\mathbf{H}$ . The spatial variation of  $\mathbf{m}_p$  depends only on the  $Z$  direction and is uniform in the  $X$ - $Y$  plane. The spin diffusion at the Py/Cu interface is taken into account as the boundary condition at  $Z = 0$ . Assuming that there is no spin relaxation at this interface, and neglecting the small difference between  $\gamma_f$  and  $\gamma_p$ , the boundary condition is expressed as<sup>6</sup>

$$\mathbf{J}_f = \mathbf{J}_p = \Gamma \left( \frac{\mathbf{M}_f - \chi_f \lambda \mathbf{M}}{\chi_f} - \frac{\mathbf{m}_p - \chi_p \mathbf{H}}{\chi_p} \right), \quad (15)$$

where  $\Gamma$  characterizes the rate of the spin diffusion at this interface.  $\mathbf{J}_p$  is the current density of the spin magnetic moment inside the Cu layer, and is given as

$$\mathbf{J}_p = -D_p \frac{\partial}{\partial Z} (\mathbf{m}_p - \chi_p \mathbf{H}). \quad (16)$$

The spin relaxation at the Cu/Pt interface or the surface of the Cu layer is also taken into account as the boundary condition at  $Z = d_{\text{Cu}}$ , which is given by<sup>28,29</sup>

$$\mathbf{J}_p = \alpha_S (\mathbf{m}_p - \chi_p \mathbf{H}). \quad (17)$$

Here,  $\alpha_S$  characterizes the rate of the spin relaxation at the Cu/Pt interface or the Cu surface.

We analyze  $\mathbf{T}$  on the linear approximation using Eqs. (11)–(17). On resonance in FMR,  $\mathbf{h}$  excites the small precession of  $\mathbf{M}$  around the equilibrium direction, which is expressed the same as that in Eq. (3). The precession of  $\mathbf{M}$  drives  $\mathbf{M}_f$  by the exchange interaction, which is given as

$$\mathbf{M}_f(t) = \chi_f \lambda \mathbf{M}(t) + \delta \mathbf{M}_f e^{-i\omega t}. \quad (18)$$

Here, the first and the second terms are the instantaneous equilibrium magnetization and the induced nonequilibrium magnetization, respectively. The induced nonequilibrium magnetization of  $\mathbf{M}_f$  diffuses from the Py to the Cu layer as the spin current described in Eq. (15), and the nonequilibrium magnetization of  $\mathbf{m}_p$  is built up inside the Cu layer, which is expressed as

$$\mathbf{m}_p(Z, t) = \chi_p \mathbf{H} + \delta \mathbf{m}_p(Z) e^{-i\omega t}. \quad (19)$$

The first and the second terms are the thermal equilibrium magnetization and the induced nonequilibrium magnetization, respectively. We take the linear combination of the rightward and the leftward propagating wave as a solution of  $\delta \mathbf{m}_p(Z)$ , which is given by

$$\delta \mathbf{m}_p(Z) = \sum_{j=+, -} (\delta m_{pj}^R e^{ik_{pj}Z} + \delta m_{pj}^L e^{-ik_{pj}Z}) \hat{\mathbf{e}}_{pj}. \quad (20)$$

Here,  $\hat{\mathbf{e}}_{pj}$  is the polarization vector of the precession given as  $\hat{\mathbf{e}}_{p\pm} = [\hat{\mathbf{x}} \mp i(\cos \beta) \hat{\mathbf{y}} \mp i(\sin \beta) \hat{\mathbf{z}}] / \sqrt{2}$  and  $\hat{\mathbf{e}}_{pz} = -(\sin \beta) \hat{\mathbf{y}} + (\cos \beta) \hat{\mathbf{z}}$ , with  $\beta \equiv \theta - \theta_H$ . Substituting Eqs. (19) and (20) into Eq. (14), one obtains the propagation constant  $k_{pj}$  given as

$$k_{p\pm}^2 = i(\omega \pm \omega_p) / D_p - l_p^{-2}, \quad (21)$$

$$k_{pz}^2 = i\omega / D_p - l_p^{-2}. \quad (22)$$

Here,  $\omega_p$  is the Larmor frequency defined as  $\omega_p \equiv \gamma_p H$ , and  $l_p$  is the spin-diffusion length for the Cu layer defined as  $l_p \equiv \sqrt{D_p \tau_p}$ . Equations (21) and (22) mean that the wavelength and the attenuating length of the propagating spin density depend on  $H$ ,  $l_p$ , and the polarization of the precession. Such a propagating mode is inherent for the transport of the precessional spin of the conduction electron,<sup>30,31</sup> and which is different from the usual spin transport, such as the current perpendicular-to-plane magnetoresistance, for which the characteristic length is  $l_p$ .<sup>32</sup> While, in the case of

$$[(\omega \pm \omega_p) \tau_p]^2 \ll 1 \quad \text{and} \quad (\omega \tau_p)^2 \ll 1, \quad (23)$$

$k_{pj}^2 = -l_p^{-2}$  is approximately obtained from Eqs. (21) and (22).<sup>33</sup> In a further analysis, we assume that Eq. (23) is satisfied for the Cu layer, for simplicity.  $\delta m_{pj}^R$  and  $\delta m_{pj}^L$  are determined from Eqs. (15)–(17) using Eqs. (18)–(20), and the relation between  $\delta \mathbf{m}_p(0)$  and  $\delta \mathbf{M}_f$  is obtained. Using its relations with Eqs. (15), (18), and (19), we obtain the following relation:

$$\mathbf{J}_f = (\Gamma_{\text{eff}} / \chi_f) \delta \mathbf{M}_f e^{-i\omega t}. \quad (24)$$

Here,  $\Gamma_{\text{eff}}$  is the effective rate of the interfacial spin diffusion modified by the dynamics and transport of  $\mathbf{m}_p$ , which is defined as

$$\Gamma_{\text{eff}}^{-1} \equiv \Gamma^{-1} + \left[ \chi_p \left( \frac{D_p}{l_p} \right) \frac{(D_p / l_p) \tanh(d_{\text{Cu}} / l_p) + \alpha_S}{(D_p / l_p) + \alpha_S \tanh(d_{\text{Cu}} / l_p)} \right]^{-1}. \quad (25)$$

Equation (24) means that the nonequilibrium magnetization induced by the precession of  $\mathbf{M}$  is lost from the Py layer on resonance of FMR. Substituting Eqs. (18) and (24) into Eq. (13) and introducing

$$\delta M_{(f)\pm} \equiv \delta M_{(f)x\pm} + i \delta M_{(f)y}, \quad (26)$$

one obtains

$$\delta M_{f\pm} = \frac{i \tau_{\text{eff}}}{1 - i(\omega \pm \omega_f) \tau_{\text{eff}}} \omega \chi_f \lambda \delta M_{\pm} \quad (27)$$

and  $\delta M_{fz} = 0$ . Here,  $\omega_f$  is defined as  $\omega_f \equiv \gamma_f \lambda M_S$ , and  $\tau_{\text{eff}}$  is the effective spin-relaxation time for the conduction electron in the Py layer, which is also defined as

$$1/\tau_{\text{eff}} \equiv 1/\tau_f + \Gamma_{\text{eff}}/\chi_f d_{\text{Py}}. \quad (28)$$

$\omega_f$  is considered to be quite large for an ordinary FM, such as Py, so that  $\omega/\omega_f \ll 1$  is sufficiently satisfied, and we assume

$$(\omega_f \tau_{\text{eff}})^{-2} \ll 1. \quad (29)$$

Taking the leading order of the real and the imaginary parts of Eq. (27) on this assumption, Eq. (27) becomes

$$\delta M_{f\pm} = (\mp 1/\omega_f + i/\omega_f^2 \tau_{\text{eff}}) \omega \chi_f \lambda \delta M_{\pm}. \quad (30)$$

Using Eqs. (12), (18), (26), and (30), one obtains the following expression for  $\mathbf{T}$ :

$$\mathbf{T} = \frac{\chi_f \lambda}{\gamma_f} \frac{d\mathbf{M}}{dt} - \frac{\chi_f \tau_{\text{eff}}^{-1}}{(\gamma_f M_S)^2} \mathbf{M} \times \frac{d\mathbf{M}}{dt}. \quad (31)$$

The first and the second terms are the additional terms of the gyromagnetic ratio (the so-called  $g$  shift), and Gilbert damping, respectively. Substituting Eq. (31) into Eq. (11), one obtains an LLG equation, which is the same as Eq. (1), by taking  $\gamma = \gamma_F$  and

$$G = G_F + \chi_f / \tau_{\text{eff}}. \quad (32)$$

Here, we used  $\chi_f \lambda \ll 1$  and  $\gamma_F / \gamma_f \approx 1$ , which are satisfied in an ordinary FM.  $\gamma$  is not influenced by the dynamics and the transport of the conduction-electron spins, so that it is independent of  $d_{\text{Py}}$  and  $d_{\text{Cu}}$ . In the case of  $G_F = 0$  and  $\tau_{\text{eff}} = \tau_f$ , Eq. (32) is in accord with the previous theory for Gilbert damping of bulk FM based on the  $s$ - $d$  model.<sup>34</sup> Using Eqs. (25), (28), and (32),  $G$  is rewritten as

$$G = G_{\text{Py}} + G', \quad (33)$$

where  $G_{\text{Py}}$  is the Gilbert damping coefficient for the bulk Py, which is defined as  $G_{\text{Py}} \equiv G_F + \chi_f / \tau_f$ , and  $G'$  is the interfacial contribution of  $G$ , which is defined as

$$G' \equiv \Gamma_{\text{eff}} / d_{\text{Py}}. \quad (34)$$

Here,  $\chi_f$  was canceled out, so that  $G'$  is independent of the properties inside the Py layer.  $G'$  increases with decreasing  $d_{\text{Py}}$ , so that  $G'$  is not negligible for a very thin Py layer. In the case that  $d_{\text{Cu}}$  is sufficiently small, Eq. (34) becomes

$$G' = [\Gamma^{-1} + (\chi_p \alpha_S)^{-1}]^{-1} / d_{\text{Py}}, \quad (35)$$

taking  $d_{\text{Cu}} \ll l_p$  in Eq. (25). The magnitude of  $G'$  is governed by the rate of the spin diffusion at the Py/Cu interface and the relaxing rate of spin at the Cu/Pt interface or the Cu surface. If the spin relaxation at the Cu/Pt interface is infinitely strong, namely  $\alpha_S^{-1} \rightarrow 0$ , Eq. (35) becomes  $G' = \Gamma / d_{\text{Py}}$ . This means that the Cu layer in contact with the Pt layer operates as a spin sink. In the case of no spin relaxation at the Cu surface, namely  $\alpha_S = 0$ ,  $G'$  becomes zero, because the spin diffusion from the Py to the Cu layer is balanced on that from the Cu to the Py layer. On the other hand, in the case of  $d_{\text{Cu}} \gg l_p$ ,  $G'$  is expressed as

$$G' = [\Gamma^{-1} + (\chi_p D_p / l_p)^{-1}]^{-1} / d_{\text{Py}}.$$

The spin relaxation at the Cu/Pt interface or the Cu surface is not operative in this regime because spin cannot diffuse beyond  $l_p$  inside the Cu layer. Instead of  $\alpha_S$ ,  $G'$  is influenced by the bulk spin relaxation of Cu, namely,  $\tau_p$  involved in  $l_p$ .

In order to quantitatively examine this model, the calculated  $G$  vs  $d_{\text{Cu}}$  was fitted to the experimental one using Eqs. (25), (33), and (34). In the fitting, we took  $G_{\text{Py}} = 0.69 \times 10^8 \text{ s}^{-1}$ , which corresponded to the value of  $G$  for Cu/Py/Cu (100 Å) film, and  $\chi_p \approx 9.8 \times 10^{-7}$  in cgs unit. The value of  $\chi_p$  was estimated from  $\chi_p = \mu_B^2 3n / 2E_F$  on the free-electron model using an electron density  $n \approx 8.5 \times 10^{22} \text{ cm}^{-3}$  and a Fermi energy  $E_F = 7 \text{ eV}$  for Cu.<sup>35</sup> Furthermore,  $\alpha_S$  for the Cu surface was taken to be zero in the fitting for Cu/Py/Cu films, because  $\alpha_S$  for the Cu surface is considered to be negligibly small.<sup>36</sup> The remaining unknown parameters are  $D_p$ ,  $l_p$ ,  $\Gamma$ , and  $\alpha_S$  for the Cu/Pt interface. The values of  $D_p$  and  $l_p$  can be determined almost independently from the fitting. While, the value of  $\Gamma$  and  $\alpha_S$  for the Cu/Pt interface cannot be obtained uniquely, because of the various combinations of the values of  $\Gamma$  and  $\alpha_S$  for the Cu/Pt interface that are allowed for the best fitting to  $G$  vs  $d_{\text{Cu}}$  for Cu/Py/Cu/Pt films. An example of the fitting is shown in Fig. 6 with the solid and the broken lines for Cu/Py/Cu/Pt and Cu/Py/Cu films, respectively. The fitting shown in Fig. 6 was performed taking  $\alpha_S^{-1} \rightarrow 0$  for the Cu/Pt interface and regarding  $D_p$ ,  $l_p$ , and  $\Gamma$  as adjustable parameters. The calculated  $G$  vs  $d_{\text{Cu}}$  is well fitted to the experimental data. From this fitting, the values of  $D_p$ ,  $l_p$ , and  $\Gamma$  were obtained to be  $120 \pm 20 \text{ cm}^2/\text{s}$ ,  $2000 \pm 500 \text{ Å}$ , and  $30 \pm 5 \text{ cm/s}$ , respectively. In the case of a fitting taking  $\Gamma^{-1} \rightarrow 0$  and adjusting the values of  $D_p$ ,  $l_p$ , and  $\alpha_S$  for the Cu/Pt interface, we obtained the result of the fitting and the values of  $D_p$  and  $l_p$  were the same as those in Fig. 6, and  $\alpha_S$  for the Cu/Pt interface was  $3 \pm 0.5 \times 10^7 \text{ cm/s}$ . Thus, although we cannot obtain the exact values of  $\Gamma$  and  $\alpha_S$  for the Cu/Pt interface, they are restricted as  $\Gamma \geq 30 \text{ cm/s}$  and  $\alpha_S \geq 3 \times 10^7 \text{ cm/s}$  for the Cu/Pt interface for the best fitting.  $D_p$  for the bulk-Cu on the free-electron model is estimated to be  $\approx 160 \text{ cm}^2/\text{s}$  from  $D_p = v_p \Lambda_p / 3$  using the Fermi velocity  $v_p \approx 1.6 \times 10^8 \text{ cm/s}$  and the mean free path  $\Lambda_p \approx 300 \text{ Å}$ .<sup>35</sup> The typical reported values of  $l_p$  are  $\approx 4500 \text{ Å}$  at 4.2 K in Ref. 25 or  $\approx 3500 \text{ Å}$  at RT in Ref. 26. The values of  $D_p$  and  $l_p$  obtained from the fitting are consistent with the above referred values, taking

into consideration the influence on  $D_p$  and  $l_p$  of the ordinary and the spin-orbit scattering by defects and phonon.<sup>37</sup> From the kinetic argument based on the free-electron model,  $\alpha_S$  is considered to be expressed as  $\alpha_S = v_p \epsilon / 2(1 - \epsilon)$ .<sup>28,29</sup> Here,  $\epsilon$  is the probability of the spin-flip reflection at an interface or a surface. For the Cu/Pt interface,  $\epsilon \geq 0.3$  is estimated from  $\alpha_S \geq 3 \times 10^7 \text{ cm/s}$  using this relation and  $v_p \approx 1.6 \times 10^8 \text{ cm/s}$ . The lower limit of  $\epsilon$  is considered to be evaluated roughly from  $\sigma_r / \sigma_{sf}$ , where  $\sigma_r$  and  $\sigma_{sf}$  are the cross section of the resistivity and the spin-flip scattering for an impurity atom in a host metal, respectively.  $\sigma_r / \sigma_{sf}$  for a Pt atom in Cu is evaluated to be  $\approx 0.1$ ,<sup>25,38</sup> so that  $\epsilon \geq 0.3$  is a reasonable estimate.  $\Gamma \geq 30 \text{ cm/s}$  at the Py/Cu interface in our films is also roughly consistent with  $\Gamma \approx 15 \text{ cm/s}$  estimated from the best value of  $\Gamma' / \chi_p = 1.5 \times 10^7 \text{ cm/s}$  in Ref. 6 taking  $\Gamma' = \Gamma$  and  $\chi_p \approx 9.8 \times 10^{-7}$ . In addition, according to a microscopic calculation of  $\Gamma$ ,<sup>39</sup>  $\Gamma$  for NM/NM tunnel junction is given as  $\Gamma = \xi(\mu_B / e)^2 R^{-1}$ , where  $e$  is the electron charge and  $R$  is the junction resistance at the NM/NM interface. If this relation is valid for a metallic contact of FM/NM in our case,  $\Gamma \geq 30 \text{ cm/s}$  leads to  $R \leq 1 \text{ f}\Omega \text{ m}^2$  from this relation, which is also consistent with  $R = 0.5 \text{ f}\Omega \text{ m}^2$  for the sputtered Py/Cu/Py films.<sup>40</sup>

This model also agrees with the experimental data, except for the fitting of  $G$  vs  $d_{\text{Cu}}$ . It is expected from Eq. (35) that the difference of  $\Delta H_{pp}$  between Cu/Py/Cu/Pt and Cu/Py/Cu films increases as  $d_{\text{Py}}$  decreases in the thinner regime of  $d_{\text{Cu}}$  as in Fig. 3(b). In addition, this model provides a natural explanation for the experimental fact that  $G$  for Cu/Py/Cu/Cu/Pt films was not enhanced. For Cu/Py/Cu/Cu/Pt films, the spin diffusion is disturbed by the low conductive regime that possibly exists in the middle of the Cu spacer layer, so that  $G$  is considered to be same as that for Cu/Py/Cu films. Silsbee *et al.* have also reported the similar influence of oxidation or contamination at the interface on the transmitted signal of CESR for their bilayer.<sup>6</sup>

The assumption of Eq. (23) has to be self-consistently satisfied with  $\tau_p \approx 3 \times 10^{-12} \text{ s}$  estimated from  $D_p$  and  $l_p$  obtained from the fitting. In the case of  $\tau_p \approx 3 \times 10^{-12} \text{ s}$ , the approximation of Eq. (23) is crude near  $\theta_H = 0^\circ$ , because the magnitude of  $H$  becomes very large nearby this angle as shown in the insets of Figs. 5(a) and 5(b). However, this is considered to be almost ineffective for the fitting in Fig. 6, since the experimental  $G$  is mostly determined by the magnitude of  $\Delta H_{pp}$  near  $\theta_H = 90^\circ$ , as shown in Figs. 5(a) and 5(b). A check of the validity of Eq. (29) is also required because Eq. (29) is essential for deriving Eq. (31) as Gilbert type damping.<sup>34</sup>  $\omega_f$  is considered to be identical to  $2JS/\hbar$ , where  $J$  and  $S$  are the constants of the  $s$ - $d$  exchange and the average spin of the localized  $d$ -electron moment, respectively. Taking  $J = 0.4 \text{ eV}$  from Ref. 41 and  $S = 0.5$ ,  $\omega_f$  is estimated to be  $\approx 6 \times 10^{14} \text{ s}^{-1}$ .  $\tau_f$  is estimated to be  $\approx 3 \times 10^{-14} \text{ s}$  from the spin-diffusion length for Py  $l_f \approx 55 \text{ Å}$  in Ref. 40, assuming the diffusion coefficient for Py  $D_f \approx 10 \text{ cm}^2/\text{s}$ . The value of  $\Gamma_{\text{eff}} / \chi_f d_{\text{Py}}$  used in the fitting is found to be less than about  $1 \times 10^{14} \text{ s}^{-1}$  by assuming  $\chi_p = \chi_f$ . Thus, Eq. (29) is satisfied enough in the fitting.



We comment on the validity of using Eq. (13). In Ref. 6, Silsbee *et al.* had originally taken into account the spatial variation of  $\mathbf{M}_f$  using a Bloch-Torrey equation, as performed for the Cu layer. In such a case, the spatial variation of  $\mathbf{M}_f$  is characterized by the propagation constant for Py  $k_{fj}$ , which is defined by changing the index  $p$  into  $f$  in Eqs. (21) and (22) and becomes  $k_{fj}^2 \approx i\omega_f/D_f$  with  $\omega_f \gg \omega$ ,  $\tau_f^{-1}$ . This means that the propagation of  $\mathbf{M}_f$  is heavily damped in the range of  $\sqrt{2D_f/\omega_f}$ , not by the bulk spin relaxation but by the exchange interaction. In the case of  $d_{\text{Py}} \ll \sqrt{2D_f/\omega_f}$ , the spatial variation of  $\mathbf{M}_f$  can be neglected, and Eq. (13) is satisfied. Taking  $\omega_f \approx 6 \times 10^{14} \text{ s}^{-1}$  and  $D_f \approx 10 \text{ cm}^2/\text{s}$ ,  $\sqrt{2D_f/\omega_f}$  is estimated to be  $\approx 20 \text{ \AA}$ . This length is comparable to or smaller than not only  $d_{\text{Py}}$  but also the mean free path for Py. Such a rapid variation of magnetization cannot be described by the Bloch-Torrey equation.<sup>28</sup> Therefore, the validity of Eq. (13) cannot be fully justified. Further experimental and theoretical studies are needed for clarifying the validity of Eq. (13).

Our experimental result and its interpretation agreed with the microscopic theories taking into account spin current generated by the precession of magnetization in NM/FM/NM films.<sup>42,43</sup> On the other hand, Berger theoretically suggested that  $G$  was enhanced in FM/NM/FM films,<sup>1,4</sup> and this was also confirmed recently in Fe/Au/Fe films.<sup>44</sup> It is unclear whether the mechanism of the enhancement of  $G$  for Fe/Au/Fe film is essentially different from that for our films. It is likely that the roll of a thick Fe layer for Fe/Au/Fe film is the same as that of Pt layer for ours, because the relaxation for precessional spin is strongly operative in a sufficiently thick FM film because of the large  $s$ - $d$  exchange, as described above.<sup>6,43</sup> In addition, a phenomenological model describing spin dynamics and transport for FM was also suggested recently, which was somewhat different from the model used in this paper and took into account not only charge and spin current but also the cross spin relaxation

between conduction and localized spin system.<sup>45</sup> Comparison between these other reports and our result is further subject.

## VI. SUMMARY

FMR was measured for Cu/Py ( $d_{\text{Py}}$ )/Cu ( $d_{\text{Cu}}$ )/Pt films with various  $d_{\text{Cu}}$  and  $d_{\text{Py}}$  in order to clarify the effect of spin diffusion driven by the precession of magnetization on Gilbert damping.  $\Delta H_{pp}$  for Cu/Py/Cu/Pt films was very large at  $d_{\text{Cu}} = 0 \text{ \AA}$  and decreased remarkably at  $d_{\text{Cu}} = 30 \text{ \AA}$ . Above  $d_{\text{Cu}} = 30 \text{ \AA}$ , it decreased gradually with increasing  $d_{\text{Cu}}$  in the anomalously wide range of  $d_{\text{Cu}}$ . This trend became more remarkable with decreasing  $d_{\text{Py}}$ . The out-of-plane angular dependence of FMR for Cu/Py ( $30 \text{ \AA}$ )/Cu ( $d_{\text{Cu}}$ )/Pt ( $0, 50 \text{ \AA}$ ) films was measured and analyzed using an LLG equation taking into account the local variation of  $4\pi M_{\text{eff}}$ . The value of  $G$  obtained from the analysis for Cu/Py/Cu/Pt films was about twice as large as that for Cu/Py/Cu films even at  $d_{\text{Cu}} = 100 \text{ \AA}$  and decreased gradually as  $d_{\text{Cu}}$  increased. At  $d_{\text{Cu}} = 2000\text{--}3000 \text{ \AA}$ ,  $G$  for Cu/Py/Cu/Pt and Cu/Py/Cu films became the same value. We also discussed the influence of the spin diffusion driven by the precession of magnetization in FMR on  $G$  using the model proposed in the past. The calculated  $G$  vs  $d_{\text{Cu}}$  was well fitted to the experimental one, and the model explained other features of the experimental results.

## ACKNOWLEDGMENTS

We acknowledge very fruitful discussions with A. Fert, Y. Suzuki, and Y. Tserkovnyak. We also thank Y. Tserkovnyak, A. Brataas, and G. E. W. Bauer for sending their preprint. This work had been supported by the Mitsubishi foundation, the Storage Research Consortium, CREST of JST (Japan Science and Technology), and Grants-in-Aid for Scientific Research from the Ministry of Education, Science, Sports and Culture of Japan.

\*Present address: Nihon University, College of Engineering, Koriyama, Fukushima, Japan.

<sup>1</sup>L. Berger, Phys. Rev. B **54**, 9353 (1996).

<sup>2</sup>J.C. Slonczewski, J. Magn. Magn. Mater. **159**, L1 (1996).

<sup>3</sup>M. Tsoi, A.G.M. Jansen, J. Bass, W.-C. Chiang, M. Seck, V. Tsoi, and P. Wyder, Phys. Rev. Lett. **80**, 4281 (1998); J.Z. Sun, J. Magn. Magn. Mater. **202**, 157 (1999); J.A. Katine, F.J. Albert, R.A. Buhrman, E.B. Myers, and D.C. Ralph, Phys. Rev. Lett. **84**, 3149 (2000); J. Grollier, V. Cros, A. Hamzic, J.M. George, H. Jaffres, A. Fert, G. Faini, J. Ben Youssef, and H. Legall, Appl. Phys. Lett. **78**, 3663 (2001).

<sup>4</sup>L. Berger, Phys. Rev. B **59**, 11 465 (1999); L. Berger, J. Appl. Phys. **90**, 4632 (2001).

<sup>5</sup>A. Jánossy and P. Monod, Solid State Commun. **18**, 203 (1976).

<sup>6</sup>R.H. Silsbee, A. Jánossy, and P. Monod, Phys. Rev. B **19**, 4382 (1979).

<sup>7</sup>P.D. Sparks and R.H. Silsbee, Phys. Rev. B **35**, 5198 (1987).

<sup>8</sup>Z. Frait and D. Fraitová, in *Spin Waves and Magnetic Excitations*, edited by A.S. Borovik-Romanov and S.K. Sinha (North-Holland, Amsterdam, 1988), Pt. 2, Chap. 1, p. 1; B. Heinrich and

J.F. Cochran, Adv. Phys. **42**, 523 (1993).

<sup>9</sup>F. Schreiber, J. Pflaum, Z. Frait, Th. Mühge, and J. Pelzl, Solid State Commun. **93**, 965 (1995).

<sup>10</sup>B. Heinrich, K.B. Urquhart, A.S. Arrott, J.F. Cochran, K. Myrtle, and S.T. Purcell, Phys. Rev. Lett. **59**, 1756 (1987); Z. Celinski and B. Heinrich, J. Appl. Phys. **70**, 5935 (1991); M. Farle, J. Lindner, and K. Baberschke, J. Magn. Magn. Mater. **212**, 301 (2000).

<sup>11</sup>W. Platow, A.N. Anisimov, G.L. Dunifer, M. Farle, and K. Baberschke, Phys. Rev. B **58**, 5611 (1998).

<sup>12</sup>S. Mizukami, Y. Ando, and T. Miyazaki, Jpn. J. Appl. Phys., Part 1 **40**, 580 (2001).

<sup>13</sup>S. Mizukami, Y. Ando, and T. Miyazaki, J. Magn. Magn. Mater. **226-230**, 1640 (2001).

<sup>14</sup>V. Kamberský, Can. J. Phys. **48**, 2906 (1970); V. Korenman and R.E. Prange, Phys. Rev. B **6**, 2679 (1972); L. Berger, J. Phys. Chem. Solids **38**, 1321 (1977).

<sup>15</sup>S. Mizukami, Y. Ando, and T. Miyazaki, J. Magn. Magn. Mater. **239**, 42 (2002).

<sup>16</sup>A.Z. Maksymowicz and K.D. Leaver, J. Phys. F: Met. Phys. **3**,

- 1031 (1973); A.A. Hussain, *Physica B* **162**, 321 (1990).
- <sup>17</sup>C. Chappert, K. Le Dang, P. Beauvillain, H. Hurdequint, and D. Renard, *Phys. Rev. B* **34**, 3192 (1986).
- <sup>18</sup>T.D. Rossing, *J. Appl. Phys.* **34**, 995 (1963).
- <sup>19</sup>J.K. Blum and W. Göpel, *Ber. Bunsenges. Phys. Chem.* **82**, 329 (1978); J.L. Bubendorff, J. Pflaum, E. Huebner, D. Raiser, J.P. Bucher, and J. Pelzl, *J. Magn. Magn. Mater.* **165**, 199 (1997).
- <sup>20</sup>R.D. McMichael, M.D. Stiles, P.J. Chen, and W.F. Egelhoff, Jr., *J. Appl. Phys.* **83**, 7037 (1998); R. Arias and D.L. Mills, *Phys. Rev. B* **60**, 7395 (1999).
- <sup>21</sup>D. Bastian and E. Biller, *Phys. Status Solidi A* **35**, 465 (1976).
- <sup>22</sup>J.W. Smits, H.A. Algra, U. Enz, and R.P. van Staple, *J. Magn. Magn. Mater.* **35**, 89 (1983).
- <sup>23</sup>C.E. Patton, Z. Frait, and C.H. Wilts, *J. Appl. Phys.* **46**, 5002 (1975); D. Bastian and E. Biller, *Phys. Status Solidi A* **35**, 113 (1976).
- <sup>24</sup>S.S.P. Parkin, R. Bhadra, and K.P. Roche, *Phys. Rev. Lett.* **66**, 2152 (1991); P. Bruno and C. Chappert, *ibid.* **67**, 1602 (1991); R. Coehoorn, A. De Veirman, and J.P.W.B. Duchateau, *J. Magn. Magn. Mater.* **121**, 266 (1993).
- <sup>25</sup>Q. Yang, P. Holody, S.-F. Lee, L.L. Henry, R. Loloee, P.A. Schroeder, W.P. Pratt, Jr., and J. Bass, *Phys. Rev. Lett.* **72**, 3274 (1994).
- <sup>26</sup>F.J. Jedema, A.T. Fillip, and B.J. van Wees, *Nature (London)* **410**, 345 (2001).
- <sup>27</sup>R.K. Wangsness, *Phys. Rev.* **104**, 857 (1956); V. Kamberský and C.E. Patton, *Phys. Rev. B* **11**, 2668 (1975).
- <sup>28</sup>M.B. Walker, *Phys. Rev. B* **3**, 30 (1971).
- <sup>29</sup>M.R. Menard and M.B. Walker, *Can. J. Phys.* **52**, 61 (1974).
- <sup>30</sup>M. Johnson and R.H. Silsbee, *Phys. Rev. B* **37**, 5312 (1988).
- <sup>31</sup>D.H. Hernando, Yu.V. Nazarov, A. Brataas, and G.E.W. Bauer, *Phys. Rev. B* **62**, 5700 (2000).
- <sup>32</sup>T. Valet and A. Fert, *Phys. Rev. B* **48**, 7099 (1993).
- <sup>33</sup>G.W. Graham and R.H. Silsbee, *Phys. Rev. B* **22**, 4184 (1980).
- <sup>34</sup>B. Heinrich, D. Fraitová, and V. Kamberský, *Phys. Status Solidi* **23**, 501 (1967).
- <sup>35</sup>C. Kittel, *Introduction to Solid State Physics* (Wiley, New York, 1996).
- <sup>36</sup>S. Schultz and C. Latham, *Phys. Rev. Lett.* **15**, 148 (1965); A. Stesmans, J. van Meijel, and S.P. Braim, *Phys. Rev. B* **19**, 5470 (1979).
- <sup>37</sup>R.J. Elliott, *Phys. Rev.* **96**, 266 (1954); F. Beuneu and P. Monod, *Phys. Rev. B* **13**, 3424 (1976); P. Monod and F. Beuneu, *ibid.* **19**, 911 (1979).
- <sup>38</sup>A. Fert, J.-L. Duvail, and T. Valet, *Phys. Rev. B* **52**, 6513 (1995); P. Monod and S. Schultz, *J. Phys. (Paris)* **43**, 393 (1982); J. Cottet, Ph. D. thesis, Université de Genève, Geneva, 1970.
- <sup>39</sup>G.G. Khaliullin and M.G. Khusainov, *Zh. Éksp. Teor. Fiz.* **86**, 187 (1984) [*Sov. Phys. JETP* **59**, 106 (1984)].
- <sup>40</sup>S.D. Steenwyk, S.Y. Hsu, R. Loloee, J. Bass, and W.P. Pratt, Jr., *J. Magn. Magn. Mater.* **170**, L1 (1997).
- <sup>41</sup>A. Fert and I.A. Campbell, *J. Phys. F: Met. Phys.* **6**, 849 (1976).
- <sup>42</sup>Y. Tserkovnyak, A. Brataas, and G.E.W. Bauer, *Phys. Rev. Lett.* **88**, 117601 (2002).
- <sup>43</sup>Y. Tserkovnyak (private communication).
- <sup>44</sup>R. Urban, G. Woltersdorf, and B. Heinrich, *Phys. Rev. Lett.* **87**, 217204 (2001).
- <sup>45</sup>C. Heide, *Phys. Rev. Lett.* **87**, 197201 (2001); *Phys. Rev. B* **65**, 054401 (2001).